

# Electrophysics Resource Center: **Scientific Imaging**

---

## White Paper: **Measuring Cold Object Temperatures Using Infrared Cameras**



373 Route 46, Fairfield, NJ 07004 Phone: 973-882-0211 Fax: 973-882-0997

[www.electrophysics.com](http://www.electrophysics.com)

# Measuring Cold Object Temperatures Using Infrared Cameras

## Introduction

For cold targets a LWIR or VLWIR camera is superior to MWIR. Data and calculations in support of this position are given in this paper.

## Applications

Many infrared scenes involve temperatures that fall below the temperatures measured in typical test configurations. Some examples are described below, which demonstrates the importance of cold temperature targets.

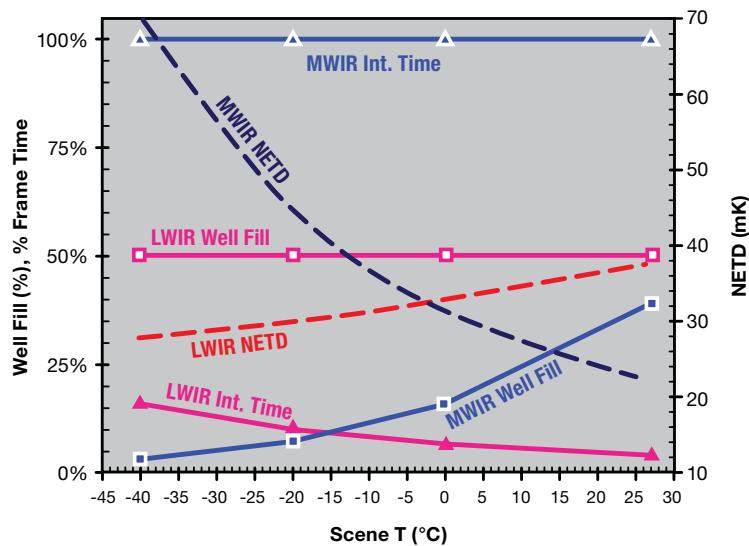
## Winter or Arctic Scenes

Cold weather infrared scenes have been modeled by NVESD as part of their key 3rd Gen FLIR initiative.

Figure 1, for a camera viewing a cold environment, shows that the LWIR well-fill remains at the desired 50% and the NETD remains good. This is not the case for MWIR, where maximum integration time is needed, and the NETD deteriorates badly as the well-fill reaches low values at low temperatures.

Figure 1. (Reference 1) U.S Army 3rd Generation Sensor Performance vs. Scene Temperature. Calculated for f/7, dual wavelength system (with supporting data from separate cameras).

Figure 1:

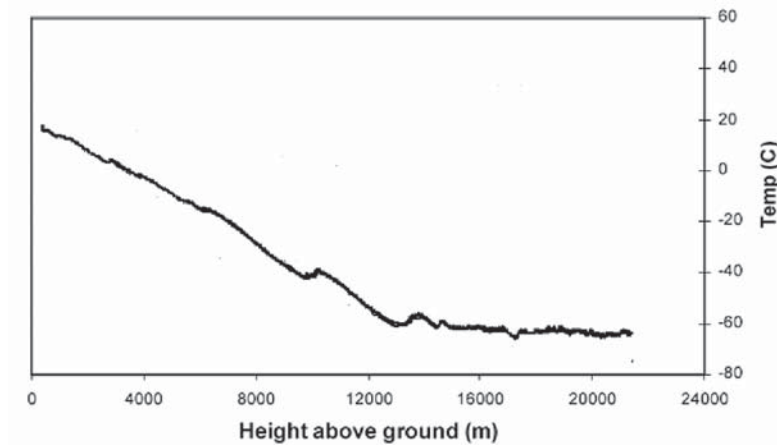


## Upper Atmospheric Targets

In the upper atmosphere, including altitudes common for aircraft, backgrounds are cold and targets can attain like temperatures.

Typical radiosonde data, shown in Figure 2, show temperatures of  $-40^{\circ}\text{C}$  at 10 km altitude.

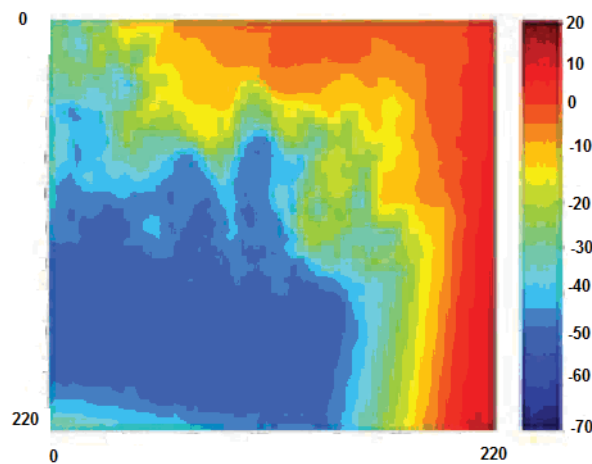
**FIGURE 2: Typical temperature data returned from an atmospheric sounding balloon**



## Cold Sky

Infrared imagery is important for tactical missile imaging systems and for imaging of toxic fumes; and such imagery must contend with the cold atmosphere. Figure 3 shows an infrared image of stratus clouds and clear sky. Apparent temperatures range from  $10^{\circ}\text{C}$  to  $-60^{\circ}\text{C}$ .

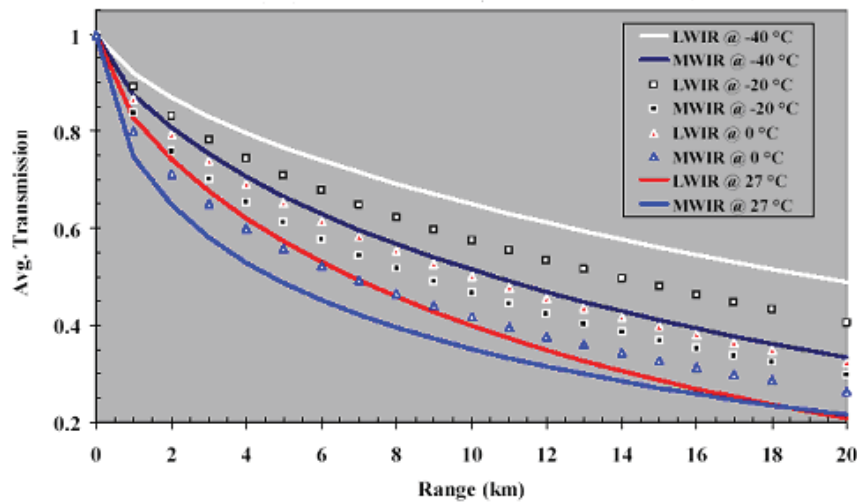
**Figure 3: (Ref. 2) Infrared image of clearing stratus clouds.**



## Long Ranges

When measuring distant targets of known temperature, a decrease in the apparent temperature of the target as a function of distance is noticeable. This effect is caused by absorption of infrared light by the air between the camera and the target, the so-called air path. The effect of the air path is particularly noticeable with infrared cameras operating in the MWIR band. This is because carbon dioxide in the atmosphere absorbs infrared light strongly in the 4.2 to 4.4 micron band. The NVESD calculations shown in Figure 4 demonstrate that LWIR has better transmission than MWIR at cold temperatures.

**Figure 4: (Ref 1) The NVESD atmospheric model clearly shows that atmospheric transmission improves with decreasing temperature, and that LWIR transmission is greater than MWIR.**



## Low Emissivity

Targets with low emissivity, which includes aerospace metals such as aluminum and titanium, exhibit low apparent temperatures, and further, can reflect the cold sky and give apparent temperatures much lower than the true value.

## I.B. Infrared Energy Overview

An ideal black substance absorbs all and reflects none of the radiant energy falling on it. Lampblack, or powdered carbon, which reflects less than 2% of the radiation falling on it, approximates an ideal black body. Since a black body is a perfect absorber of radiant energy, by the laws of thermodynamics it must also be a perfect emitter of radiation. The distribution according to wavelength of the radiant energy of a black body radiator depends on the absolute temperature of the black body and not on its internal nature or structure. As the temperature increases, the wavelength at which the energy emitted per second is a maximum decreases. This phenomenon can be seen in the behavior of an ordinary incandescent object, which gives off its maximum

radiation at shorter and shorter wavelengths as it becomes hotter and hotter. First it glows in long red wavelengths, then in yellow wavelengths, and finally in short blue wavelengths. In order to explain the spectral distribution of black body radiation, Max Planck developed the quantum theory in 1901. In thermodynamics the principle of the black body is used to determine the nature and amount of the energy emitted by a heated object.

Any body at any temperature above absolute zero will radiate to some extent, but the intensity and frequency distribution of the radiation depends on the detailed structure of the body. To make any progress in understanding radiation, we must specify the details of the body radiating. The simplest possible model is to consider a body which is a perfect absorber, and therefore the best possible emitter. For obvious reasons, this is called a “black body”. At sufficiently high temperatures, all bodies become good radiators. Items heated until they glow in a fire look much more similar than they do at room temperature. Conversely at colder temperatures objects become poor radiators particularly at the wavelengths (3-5 microns or Mid Wave and 8-12 micron or Long Wave) at which commercial infrared cameras operate.

This relationship exists because all objects are composed of continually vibrating atoms, with higher energy atoms vibrating more frequently. The vibration of all charged particles, including these atoms, generates electromagnetic waves. The higher the temperature of an object, the faster the vibration, and thus the higher the spectral radiant energy. As a result, all objects are continually emitting radiation at a rate with a wavelength distribution that depends upon the temperature of the object and its spectral emissivity,  $\epsilon$ . The energy emitted by a true blackbody is the maximum theoretically possible for a given temperature. The radiative power (or number of photons emitted) and its wavelength distribution are given by the Planck’s radiation law where  $\lambda$  is the wavelength,  $T$  is the temperature,  $h$  is Planck’s constant,  $c$  is the velocity of light, and  $k$  is Boltzmann’s constant.

$$W(\lambda, T) = \frac{2\pi hc^2}{\lambda^5} \left[ \exp\left(\frac{hc}{\lambda kT}\right) - 1 \right]^{-1} \text{ W/(cm}^2 \mu\text{m)}, \quad (1)$$

$$P(\lambda, T) = \frac{2\pi c}{\lambda^4} \left[ \exp\left(\frac{hc}{\lambda kT}\right) - 1 \right]^{-1} \text{ photons/(s cm}^2 \mu\text{m)}, \quad (2)$$

Figure 5 shows a plot of these curves for a number of blackbody temperatures. As the temperature increases, the amount of energy emitted at any wavelength increases too, and the wavelength of peak emission decreases. The latter is given by Wien's displacement law,

$$\lambda_{mw}T = 2898 \mu\text{mK} \quad \text{for maximum watts,}$$

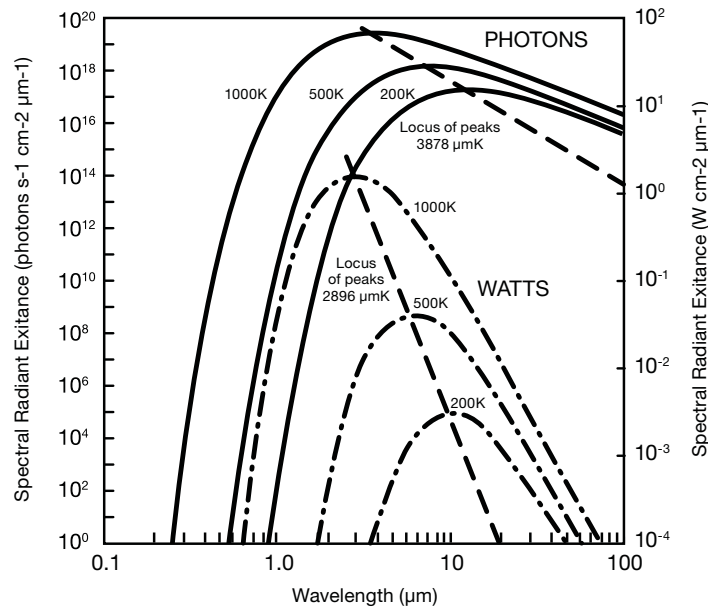
$$\lambda_{mp}T = 3670 \mu\text{mK} \quad \text{for maximum photons.}$$

The loci of these maxima are shown in Fig. 5. Note that for an object at an ambient temperature of 259 K,  $\lambda_{mw}$  and  $\lambda_{mp}$  occur at 10.0  $\mu\text{m}$  and 12.7  $\mu\text{m}$ , respectively. For hotter objects, the maximum emission occurs at shorter wavelengths. The waveband 1–15  $\mu\text{m}$  in the infrared region of the electromagnetic spectrum contains the maximum radiative emission for thermal imaging purposes.

Due to atmospheric absorption and FPA manufacturing considerations, the four common wavelength bands for cameras are SWIR (1  $\mu\text{m}$  to 3  $\mu\text{m}$ ), MWIR (3  $\mu\text{m}$  to 5  $\mu\text{m}$ ), LWIR (8  $\mu\text{m}$  to 10  $\mu\text{m}$ ) and VLWIR (8 to 12  $\mu\text{m}$ ).

As shown in this paper, the particular “window” required for imaging depends strongly on the background and target temperatures.

Figure 5: (Ref. 3) Planck's Law for Spectral Radiant Exitance



## Practical Considerations

In the infrared camera electronics chain, the blackbody energy is converted into an output signal voltage through interaction of the FPA detector elements, the readout integrated circuit and the camera external electronics. The photosignal depends on the spectral radiant exitance of the target and the characteristics of the FPA detectors: spectral band, area of detection, quantum efficiency and the solid angle of detection.. The camera and FPA optical elements, filters, windows, mirrors, and lenses affect the energy reaching the detector elements.

Integration of Planck's curves over the detector spectral response is easily performed with a Planck Calculator. The Cedip Calculator also includes the detector and system parameters needed to convert the blackbody energy to signal output. Figure 6 is a screen shot of Planck's Calculator, showing the parameters needed to calculate the expected signal. At the bottom is the result in flux (photons/s or W) and in Quantum Capacity, which is the number of electrons on the integrating capacitor for the given integration time. Then the percentage well-fill is calculated. Since a full well for 14-bit resolution is 16,384 counts, the number of expected counts is easily calculated.

**Figure 6: Planck's Calculator included with Altair software. Shown are all detector and camera parameters required for calculation of percentage well-fill.**

Planck Calculator

Detector

Type   Manual Configuration

Points / Line  0 x  0 pixels

Cut on / Cut off  7.7 -  9.5 μm

Pixel Size (t-w)  25 x  25 μm

Quantum Efficiency  70 %

Max. Capacity  37 10e6 electrons

Aperture  2  F#  sr

Optical Transmission  100 %

Atmospheric Transmission  100 %

General

Black body Temperature  -30  °C

Integration time  100  μs

Surface Emissivity  1

Results

Flux: 2.46e+010 photons/s (5.63e-010 W)

Quantum Capacity: 1.72e+006

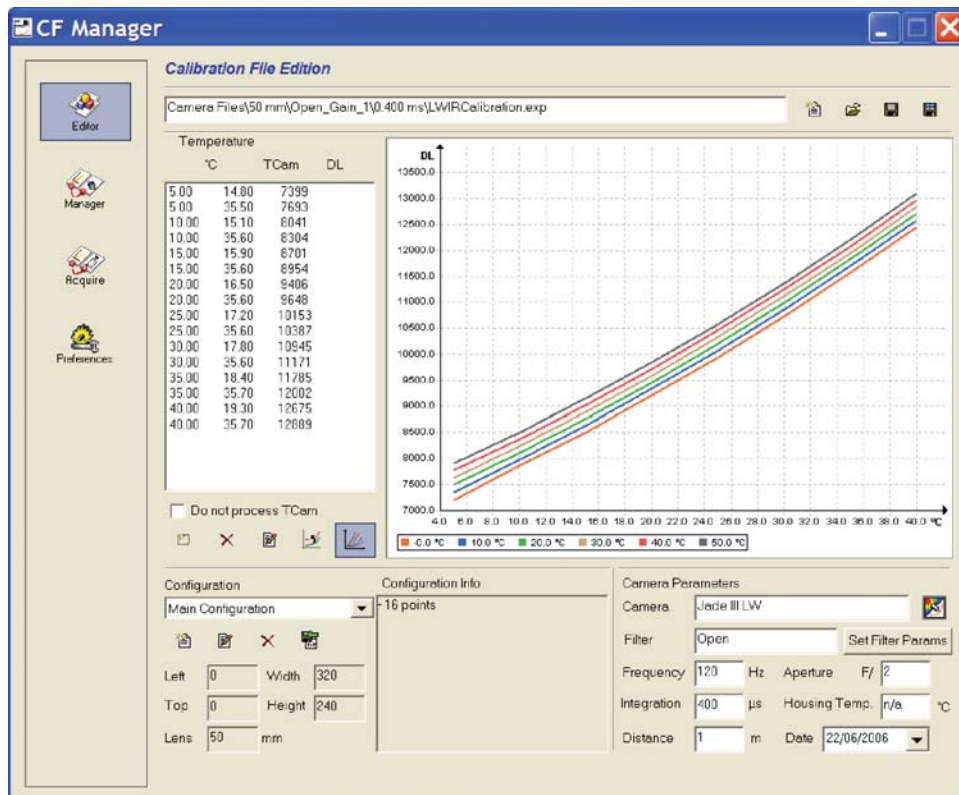
4.6 %

Because of variation of the parameters from detector to detector in a FPA, each detector gives a slightly different photosignal. Surprisingly, the detector area is important in this regard, because of etching variations during manufacture. A NUC, non-uniformity correction, eliminates these differences--a uniform scene is imaged and each detector output is corrected to yield a uniform image.

One must also correct for differences in the external camera electronics—as the camera housing changes temperature, the output can vary. The Cedip cameras are true radiometers, and automatically adjust for changes in the housing temperature.

A typical camera calibration is shown in the screen shot, Figure 7. The families of curves are for various camera housing temperatures. The camera converts a blackbody signal to DL and to absolute temperature.

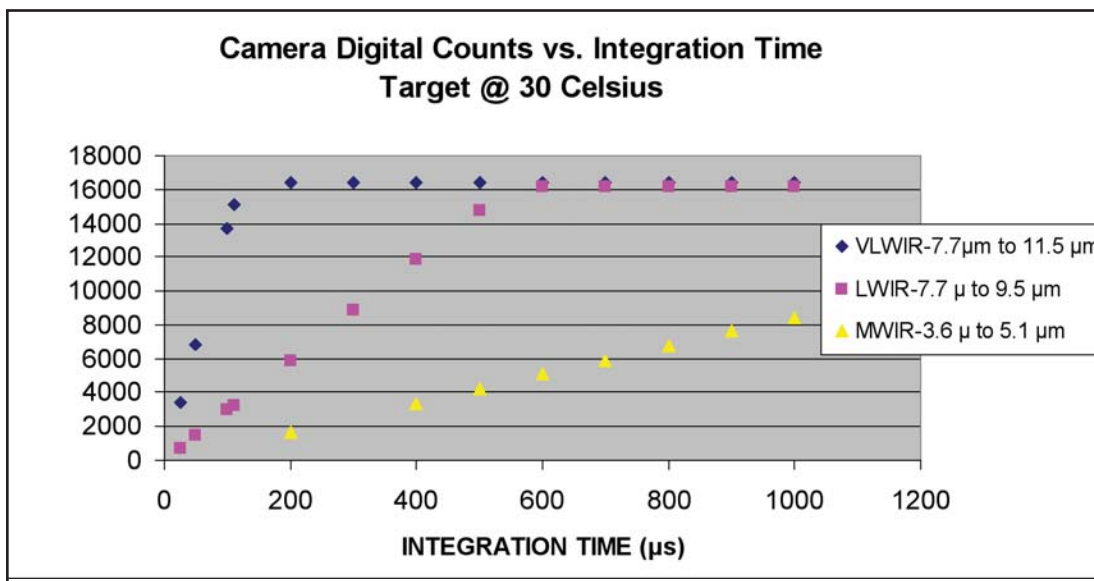
Figure 7: Typical calibration file for a Cedip LW camera. The family of curves shown are for differing camera housing temperatures.



The optimum integration time for a camera yields a digital count (DL) level that half fills the well (integrating capacitor). For a 14-bit system an operating level of about 8000 DL is desired. The signal saturates at 16,000 DL at the high end, and at the low end usually saturates at about 700 counts due to system noise.

The calculated camera counts for typical room temperature imaging are shown in Figure 8. Cedip cameras with three different cut-off wavelengths are shown: InSb MWIR with a wavelength range of 3.6  $\mu\text{m}$  to 5.1  $\mu\text{m}$ ; MCT LWIR with a wavelength range of 7.7  $\mu\text{m}$  to 9.5  $\mu\text{m}$ ; and MCT VLWIR with a wavelength range of 7.7  $\mu\text{m}$  to 11.5  $\mu\text{m}$ .

**Figure 8: Camera output, in DL, as a function of integration time, for three Cedip cameras, MWIR, LWIR and VLWIR**

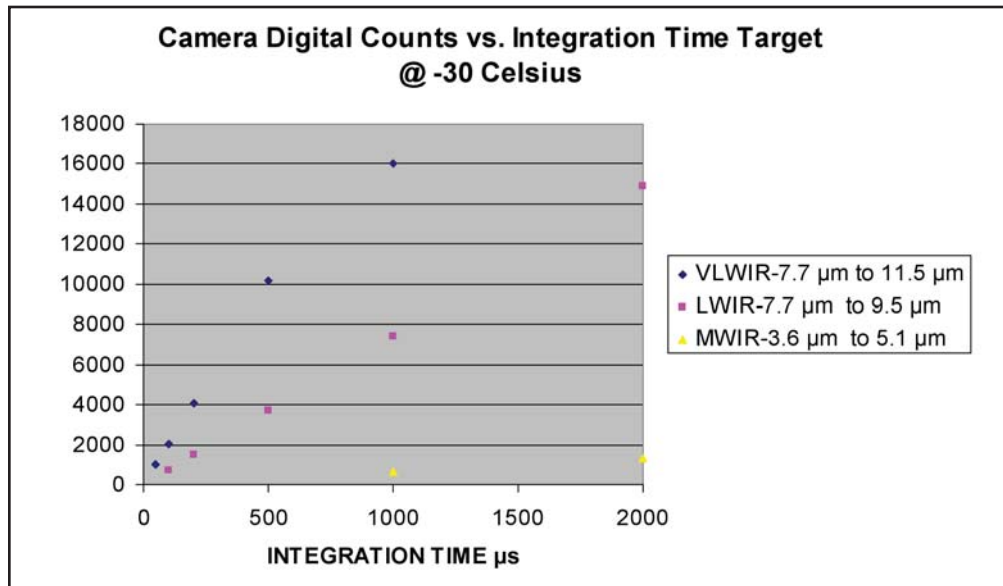


For a 30°C target, optimum integration times are 1 ms for MWIR, 300  $\mu\text{s}$  for LWIR and 60  $\mu\text{s}$  for VLWIR. MWIR cameras operate comfortably for applications at room temperature with slowly moving targets. For fast moving targets, requiring a short integration time, LWIR or VLWIR cameras are superior.

## Expected Cold Target Performance

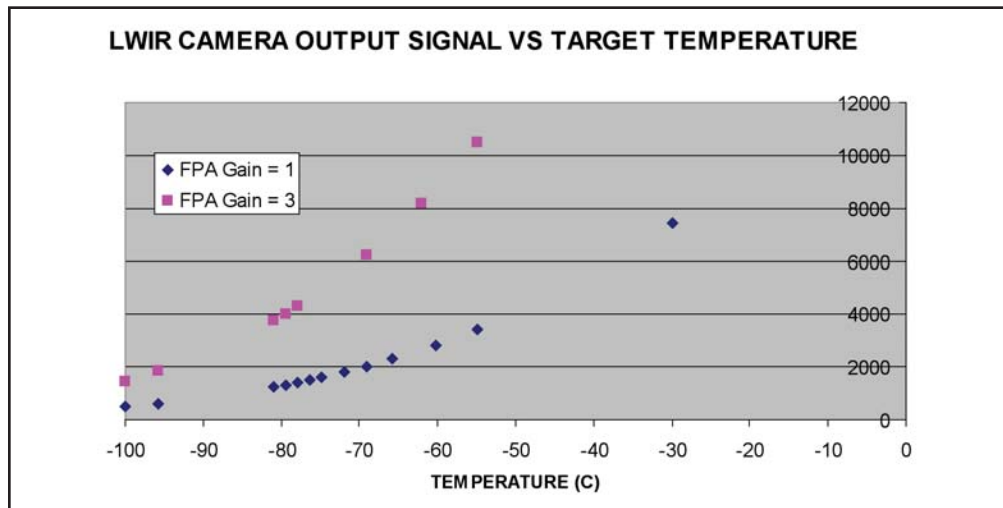
For cold target applications, as described in Section I.A., MWIR cameras quickly become starved for photocurrent, resulting in low DL. Figure 9 shows a comparison of MWIR, LWIR and VLWIR cameras at a target temperature of  $-30^\circ\text{C}$ , showing that the MWIR camera is not useful for these applications—it is completely starved for photon even at 2 ms integration time, while the LW optimum integration time is 1 ms and the VLWIR optimum is 400  $\mu\text{s}$ .

Figure 9: At cold target temperatures, the MWIR cameras are starved for photons, while LWIR and VLWIR cameras operate at reasonable integration times.



The expected performance of LWIR and VLWIR cameras at low temperatures can be examined in more detail. Figure 10 shows the expected LWIR results for target temperatures of  $-30^{\circ}\text{C}$  to  $-100^{\circ}\text{C}$ .

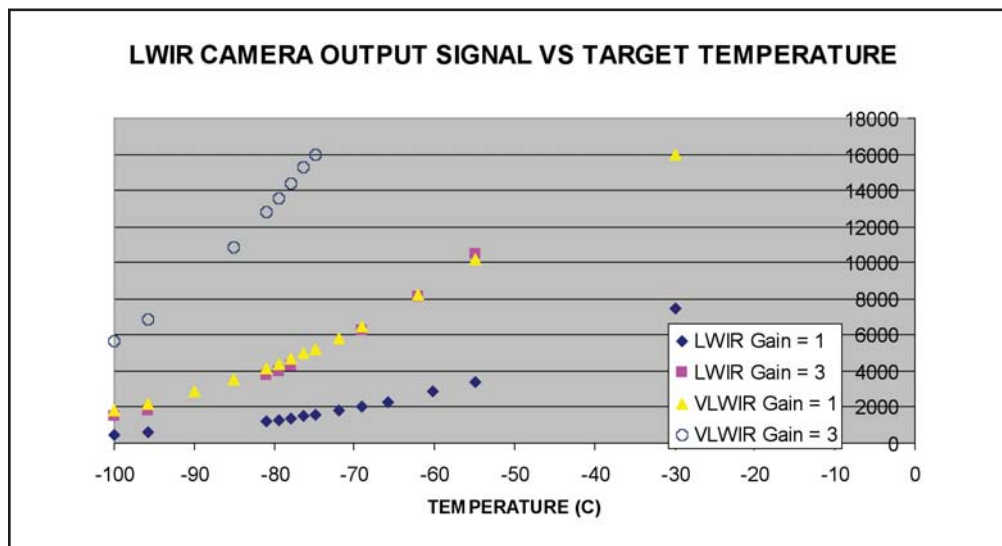
Figure 10: LWIR camera expected output at low target temperatures. Integration time = 1 ms.



Note that the LWIR camera, at its usual FPA gain of 1 ( $37\text{e}6\text{ e}^-$ ), becomes starved for photons at temperatures below  $-80^{\circ}\text{C}$ . The Sofradir FPA multiplexers have a feature that allows the FPA gain to be set by the operator to either 1 or 3 ( $12\text{e}6\text{ e}^-$ ). With Gain = 3 the camera has a DL level of 2000 at  $-95^{\circ}\text{C}$ .

Figure 11 adds the expected output for a VLWIR camera. The Gain = 1 output is about the same as the Gain = 3 for the LWIR camera. Gain = 3 for VLWIR is obviously a superior operating condition for temperatures below  $-80^{\circ}\text{C}$ . At higher temperatures the VLWIR camera can be comfortably operated at shorter integration times.

Figure 11: VLWIR and LWIR expected camera output for FPA gains of 1 and 3. Integration time = 1 ms.



## Conclusions

Cold target applications require a LWIR ( $7.7\mu\text{m}$  to  $9.5\mu\text{m}$ ) camera for optimum performance. Expected camera output levels are shown in Figure 10 for the two available FPA gains, with an integration time of 1 ms. For temperatures below  $-80^{\circ}\text{C}$ , or for cold targets at high speeds (short integration times), a VLWIR camera is advised.

## References

1. Van A. Hodgkin, Brian Kowalewski, Dave Tomkinson, Brian P. Teaney, Ted Corbin, Ronald Driggers, Modeling of IR Sensor Performance in Cold Weather U.S. Army RDECOM CERDEC Night Vision and Electronic Sensors Directorate
2. Joseph A. Shaw, Remote Sensing Systems Overview, Montana State University, class notes
3. A. Rogalski\*1 and K. Chrzanowski, Opto-Electronics Review 10(2), 111-136 (2002)

For more comprehensive White Papers  
visit our online Knowledge Center.  
**[www.electrophysics.com/infrared-cameras](http://www.electrophysics.com/infrared-cameras)**



373 Route 46, Fairfield, NJ 07004 Phone: 973-882-0211 Fax: 973-882-0997  
[www.electrophysics.com](http://www.electrophysics.com)

© 2009 Electrophysics Corp. All rights reserved.  
An ISO 9001 Certified Company.